Biochemical and Biophysical Research Communications 429 (2012) 137–141

Contents lists available at SciVerse ScienceDirect

Biochemical and Biophysical Research Communications

journal homepage: www.elsevier.com/locate/ybbrc

Different Ca^{2+}-sensitivities between the EF-hands of T- and L-plastins

Takuya Miyakawa [a], Hiroto Shinomiya [b], Fumiaki Yumoto [a,c], Yumiko Miyauchi [a], Hiroyuki Tanaka [d], Takao Ojima [d], Yusuke S. Kato [a,e,*], Masaru Tanokura [a,*]

[a] Department of Applied Biological Chemistry, Graduate School of Agricultural and Life Sciences, The University of Tokyo, Bunkyo-ku, Tokyo 113-8657, Japan
[b] Ehime Prefectural Institute of Public Health and Environmental Science, Matsuyama, Ehime 790-0003, Japan
[c] Department of Cell Physiology, The Jikei University School of Medicine, Minato-ku, Tokyo 105-8461, Japan
[d] Laboratory of Marine Biotechnology and Microbiology, Graduate School of Fisheries Sciences, Hokkaido University, Hakodate, Hokkaido 041-8611, Japan
[e] Institute for Health Sciences, Tokushima Bunri University, Tokushima 770-8514, Japan

ARTICLE INFO

Article history:
Received 24 October 2012
Available online 7 November 2012

Keywords:
Plastin
Calcium
EF-hand motif
Conformational change
NMR
Isothermal titration calorimetry

ABSTRACT

Plastins are Ca^{2+}-regulated actin-bundling proteins, and essential for developing and stabilizing actin cytoskeletons. T-plastin is expressed in epithelial and mesenchymal cells of solid tissues, whereas L-plastin is expressed in mobile cells such as hemopoietic cell lineages and cancer cells.

Using various spectroscopic methods, gel-filtration chromatography, and isothermal titration calorimetry, we here demonstrate that the EF-hand motifs of both T- and L-plastin change their structures in response to Ca^{2+}, but the sensitivity to Ca^{2+} is lower in T-plastin than in L-plastin. These results suggest that T-plastin is suitable for maintaining static cytoskeletons, whereas L-plastin is suitable for dynamic rearrangement of cytoskeletons.

1. Introduction

The actin cytoskeleton is an essential component of all eukaryotic cells and is involved in diverse cellular events such as cellular motion, division and adhesion, as well as in the control of cell shape [1,2]. Dynamic rearrangement of the actin cytoskeleton is required in immune responses such as T-cell receptor signaling, chemotactic and adhesive responses critical to normal leukocyte trafficking and motility, and phagocytosis and intracellular killing of pathogens [3]. While many actin-binding proteins regulate the recruitment and stabilization of the actin cytoskeleton, recent studies have implicated the actin-bundling protein, L-plastin, as a critical regulator of actin dynamics in cells of both the adaptive and innate immune systems. L-plastin is expressed in hemopoietic cell lineages and in many types of cancer cells [4–8]. The expression of L-plastin is dependent on the transformation to cancer cells, and may be related to the cells' acquisition of the capability to migrate and invade, as in the case of leukocytes. In contrast, the T-plastin isoform is constitutively expressed in epithelial and mesenchymal cells of solid tissues to organize the F-actin networks in those cells [5–8].

Plastins including the L- and T-isoforms are composed of two EF-hand motifs and two actin-binding domains (ABDs) [8,9]. ABD is also seen in a wide variety of actin-binding proteins such as α-actinin, spectrin, cortexillin, and dystrophin [10]. A single ABD is composed of two tandemly arranged CH domains in a single polypeptide chain, i.e., four CH domains are sequentially arranged in plastins. This arrangement is important for the actin-bundling activity of plastins [11].

The EF-hand motif is a well known Ca^{2+}-binding motif found in calmodulin, troponin, and other calcium-sensing proteins [12]. The general function of an EF-hand motif is to chelate a Ca^{2+} ion for converting intracellular Ca^{2+} signals to protein–protein interaction, to carry out various cellular events. The EF-hand motifs in the plastin isoforms are involved in the regulation of the actin-bundling activity of plastins [13–15]. Increased concentration of cellular Ca^{2+} inhibits the formation of actin bundles formed by plastins [16,17].

As mentioned above, plastins have isoforms that are expressed in different cell types. However, it remains unclear why the expression of the plastin isoforms is cell-type-dependent. To address this,

Abbreviations: ABD, actin-binding domain; CH domain, calponin-homology domain; ITC, isothermal titration calorimetry; EF^T, the EF-hand motifs of T-plastin; EF^L, the EF-hand motifs of L-plastin; CD, circular dichroism; NMR, nuclear magnetic resonance; pCa, the negative decadic logarithm of the calcium ion concentration; pCa_{50}, the pCa value at half-maximal fluorescence change; $[Ca^{2+}]_i$, the intracellular concentration of Ca^{2+}.

* Corresponding authors. Addresses: Department of Applied Biological Chemistry, Graduate School of Agricultural and Life Sciences, The University of Tokyo, 1-1-1 Yayoi, Bunkyo-ku, Tokyo 113-8657, Japan (M. Tanokura), Institute for Health Sciences, Tokushima Bunri University, 180 Nishihama, Yamashiro-cho, Tokushima 770-8514, Japan (Y.S. Kato). Fax: +81 3 5841 8023 (M. Tanokura).

E-mail addresses: ysk@tks.bunri-u.ac.jp (Y.S. Kato), amtanok@mail.ecc.u-tokyo.ac.jp (M. Tanokura).

0006-291X/$ - see front matter © 2012 Elsevier Inc. All rights reserved.
http://dx.doi.org/10.1016/j.bbrc.2012.10.126

we here focus on the EF-hand motifs of T- and L-plastins to reveal the functional difference of these isoforms, since a comparison of the protein sequences revealed that the identity in the EF-hand regions between the isoforms (~55%) is much lower than that in the ABD regions (~85%).

2. Materials and methods

2.1. Protein preparation

The cDNAs encoding the EF-hand motifs of T- and L-plastins (EF^T and EF^L, respectively) were amplified by PCR. The NCBI accession numbers of the template sequences were AB182243 and NM_008879, which are the sequences of murine plastins. The sequences of the PCR primers were as follows: 5′-CATATGGATGAGATGGCGACCACC-3′ and 5′-GAATTCTTAAATCCCTTCTTTCCTGTTGATGGC-3′ for EF^T; 5′-CATATGGCCAGAGGATCCGTGTCTGACG-3′ and 5′-GAATTCTTAGATCCCTTCCTTCTTGTTGATAGC-3′ for EF^L. The amplified fragments were ligated into a modified pET28a vector (Merck, Rahway, NJ), which has a 6× His-tag and TEV protease cleavage site. 6× His-tagged EF^T and EF^L were expressed in *Escherichia coli* BL21(DE3) (Merck). The proteins were purified using Ni–NTA agarose (Qiagen, Venlo, Netherlands). The 6× His-tag was removed by AcTEV Protease (Life Technologies, Carlsbad, CA). Contaminating Ca^{2+} was removed by trichloroacetic acid treatment [18]. The proteins used for the ITC measurements were further reduced by 5 mM DTT and purified by Resource-Q and Superdex 75 columns (GE Healthcare, Buckinghamshire, UK).

2.2. CD measurements

CD spectra were recorded on a J-720 spectropolarimeter (Jasco, Tokyo, Japan) at room temperature. The solution compositions were 20 μM EF^T (or EF^L), 100 mM KCl, 50 μM EDTA, and 20 mM Mops-KOH (pH 7.0) for the Ca^{2+}-free state; and 20 μM EF^T (or EF^L), 100 mM KCl, 10 mM $CaCl_2$, and 20 mM Mops-KOH (pH 7.0) for the Ca^{2+}-bound state.

2.3. Analytical gel filtration experiments

Gel filtration experiments were performed using an ÄKTA explorer 10S (GE Healthcare) and a Superdex 75 10/30 column (GE Healthcare) equilibrated with 120 mM KCl, 50 μM EDTA, and 20 mM Mops-KOH (pH 7.0) for the Ca^{2+}-free condition. 50 μM EDTA was replaced with 10 mM $CaCl_2$ for the Ca^{2+}-bound condition. 20 μM EF^T and EF^L in the equilibration buffer were applied to the column.

2.4. NMR spectroscopy

^{15}N-labeled EF^T and EF^L were produced by culturing the expression systems in modified M9 media with $^{15}NH_4Cl$ (SI Science, Saitama, Japan). ^1H–^{15}N HSQC experiments were performed with an Inova 600 spectrometer (Agilent Technologies, Palo Alto, CA) equipped with Cold Probe (Agilent Technologies). The compositions of the calcium-free sample solution were as follows: 0.1 mM ^{15}N-labeled EF^T (or EF^L), 10% ^2H_2O, 5 mM Mops-KOH, 50 μM EDTA, 5 mM DTT, and 100 mM KCl at pH 6.7. In the Ca^{2+}-bound condition, 50 μM EDTA was replaced with 10 mM $CaCl_2$. All the data were processed and displayed using NMRPipe/NMRDraw [19].

2.5. Fluorescence spectroscopy

Fluorescence data were recorded on an RF-5300PC spectrofluorometer (Shimadzu, Kyoto, Japan). Excitation was performed at 278 nm while emission was monitored at 334 nm to measure the Tyr fluorescence. The solution compositions were 20 μM EF^T (or EF^L), 20 mM Mops-KOH (pH 7.0), 100 mM KCl, 1 mM DTT, and various concentration of $CaCl_2$. To determine the pCa values at half-maximal fluorescence changes (pCa_{50}), plots of the relationship between relative fluorescence change and calcium concentration, pCa, were fitted to sigmoidal dose–response curves by nonlinear regression using GraphPad Prism Version 3.00 for Windows (GraphPad Software, San Diego, CA).

2.6. ITC measurements

ITC was performed at 25 °C on an iTC_{200} microcalorimeter (GE Healthcare). EF^T and EF^L were dialyzed against 10 mM Pipes-KOH (pH 6.8), 150 mM KCl, and 1 mM 2-mercaptoethanol. The outer dialysate was used as a solvent to prepare the $CaCl_2$ solution. The sample cell was filled with 100 μM protein solution and titrated with the solution containing 1.6 mM $CaCl_2$. For each titration, 26 consecutive 1.5 μL aliquots of the $CaCl_2$ solution were injected at 120 s intervals. The heat of sample dilution was obtained from a final injection in the presence of a 2.7-fold molar excess of Ca^{2+} over EF^T and EF^L, and was subtracted from the Ca^{2+}-binding isotherm. Data analysis was performed using the Origin-ITC analysis package (GE Healthcare) in "one set of sites" or "two set of sites" modes. The appropriateness of the modes was evaluated by the χ^2 value of curve fitting.

3. Results

3.1. Secondary structure change in EF^L upon Ca^{2+}-binding

We first produced the EF-hand constructs of T- and L-plastins (EF^T and EF^L, respectively) to compare the secondary structure contents using CD. All of the spectra of EF^T and EF^L showed two negative peaks around 208 and 222 nm (Fig. 1), which suggests that both EF^T and EF^L are α-helix-rich. This is consistent with the characteristics of the other EF-hand proteins [12]. The CD analysis also showed that the spectrum change of EF^T was almost negligible with addition of 10^{-2} M Ca^{2+}, whereas that of EF^L was obvious. This suggests that EF^L changes the secondary structure content upon the addition of Ca^{2+}. In contrast, it appears that the secondary structure change in EF^T was slight upon the addition of Ca^{2+}. Typical EF-hand proteins change the conformations with the increase of Ca^{2+} concentration, as chelating of Ca^{2+} opens the angle between the α-helices in EF-hands, so the results of EF^T were unexpected.

3.2. EF^T also changes the conformation with Ca^{2+}

Our next question is whether the higher order structure of EF^T changes or not upon addition of Ca^{2+}. To answer this question, we carried out analytical gel filtration chromatography and NMR. The results of the gel filtration experiments showed that the elution time of EF^T was delayed in the Ca^{2+}-bound condition, compared with the Ca^{2+}-free condition (Fig. 2A). This suggests that the molecular radius of EF^T became smaller with Ca^{2+}. The elution time of EF^L was similarly delayed with the addition of Ca^{2+} (Fig. 2B). NMR spectra of EF^T and EF^L also showed that numerous signals derived from both of the proteins moved in the 2D spectra upon addition of Ca^{2+} (Fig. 2C and D). This indicates that magnetic environments of such numerous amino acid residues were perturbed by the addition of Ca^{2+}. The data from the gel filtration and NMR analyses together suggest that EF^T as well as EF^L changes the tertiary structure upon Ca^{2+}-binding.

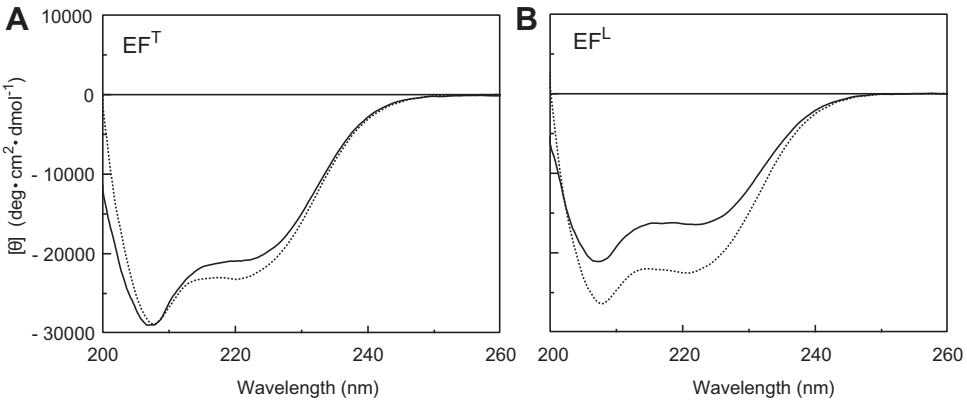

Fig. 1. Changes in secondary structure contents by Ca^{2+}. The CD spectra of EF^T (A) and EF^L (B) in the apo (solid line) and Ca^{2+}-bound (dashed line) states are shown.

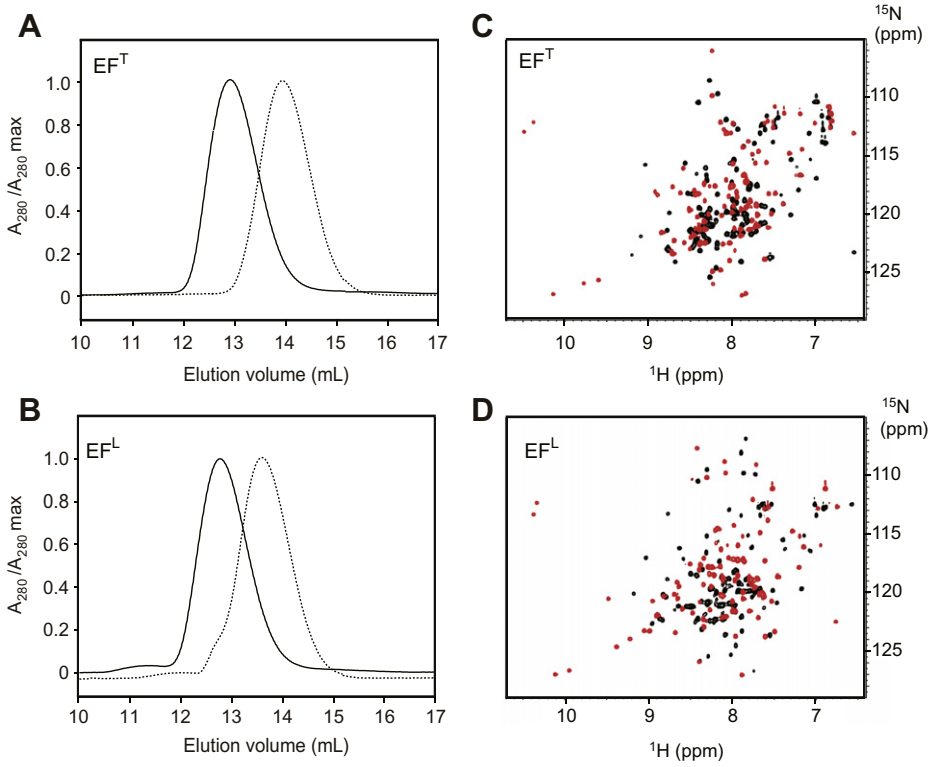

Fig. 2. Changes in tertiary structure by Ca^{2+}. Gel filtration chromatograms of EF^T (A) and EF^L (B) in the apo (solid line) and Ca^{2+}-bound (dashed line) states are shown. These figures show changes in the molecular radiuses of EF^T and EF^L in response to Ca^{2+}. The elution volumes of the apo and Ca^{2+}-bound forms of EF^T were 12.9 and 14.0 mL, respectively, whereas those of EF^L were 12.8 and 13.6 mL. ^1H-^{15}N HSQC spectra of EF^T (C) or EF^L (D) in the apo (black) and Ca^{2+}-bound (red) states. Structural changes of EF^T and EF^L are monitored by 2D NMR. To assess the effects of Ca^{2+} on the tertiary structures of EF^T and EF^L, we measured 2D NMR using uniformly ^{15}N-labeled EF^T and EF^L. All signals in the spectra are from amide groups in the proteins. The spectra under all the conditions show highly dispersed sharp signals, indicating that the proteins are properly folded without aggregation. The formation of aggregation would broaden the signals. Differences in the distribution of the signals between the presence and absence of Ca^{2+} indicate the change in the tertiary structure.

3.3. A higher concentration of Ca^{2+} is required for the structural change of EF^T

Fluorescent measurements were carried out by exploiting fluorescence from the intrinsic Tyr residues of EF^T and EF^L to measure the structural changes of these proteins (Fig. 3). Addition of Ca^{2+} to the protein solution causes an increase in the fluorescence. This is because the structural change around the Tyr residues changes the fluorescent characteristics of those proteins. The sigmoidal curves show the difference in the apparent Ca^{2+}-binding strength between EF^T and EF^L. The pCa_{50} values of EF^T and EF^L were 4.81 ± 0.04 (15.4 μM in molar concentration) and 5.53 ± 0.07 (2.95 μM), respectively. This suggests that the structural change of EF^T requires higher concentration of Ca^{2+} than that of EF^L.

3.4. ITC measurements

To directly observe the Ca^{2+}-binding of EF^T and EF^L, we carried out ITC measurements (Supplementary Fig. S1). The Ca^{2+}-binding of EF^T and EF^L was exothermic. The obtained parameters are summarized in Table 1. The K_d values for the affinity to Ca^{2+} were 0.37 (N = 1.14) and 10.6 μM (N = 0.87) for the Ca^{2+}-binding sites in EF^T.

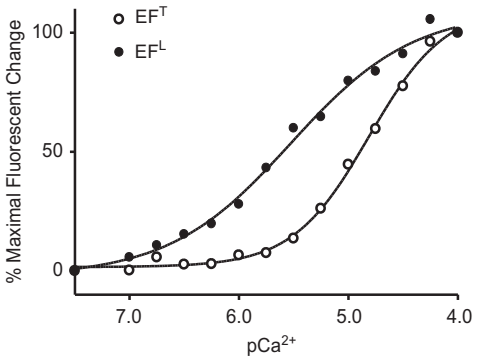

Fig. 3. Fluorescence measurements. Ca^{2+}-dependent fluorescence changes of EF^T (open circles) and EF^L (filled circles) are shown. The relative fluorescence changes of EF^T and EF^L versus pCa were plotted. Sigmoidal curves were fitted to the plots to calculate the apparent Ca^{2+} binding strength of EF^T and EF^L.

Table 1
Thermodynamic parameters of EF^T and EF^L obtained by ITC measurements. Reaction enthalpies (ΔH), dissociation constants (K_d), and stoichiometry (N) were determined directly from curve-fitting to the ITC thermogram (Supplementary Fig. S1). The changes in the Gibbs free energy (ΔG) and entropy (ΔS) were determined by using the equation $\Delta G = -RT\ln K_a = \Delta H - T\Delta S$, where R and T are the universal gas constant and absolute temperature, respectively.

	K_d (μM)	N	ΔG (kcal/mol)	ΔH (kcal/mol)	ΔS (cal/mol/K)
EF^{Ta}	10.6 ± 1.4	0.87 ± 0.05	−6.79 ± 0.28	−2.26 ± 0.28	15.2
EF^{Tb}	0.37 ± 0.42	1.14 ± 0.11	−8.79 ± 0.04	−2.77 ± 0.04	20.2
EF^L	1.05 ± 0.08	1.84 ± 0.01	−8.15 ± 0.02	−4.39 ± 0.02	12.6

[a] The low affinity site.
[b] The high affinity site.

These findings suggest that EF^T has two Ca^{2+}-binding sites with different binding affinity. One of those should be defined as a low affinity site, whereas the other should be considered a high affinity site [20]. In contrast, the K_d values were 1.05 μM for both Ca^{2+}-binding sites in EF^L, because N for this binding equaled ~2. This suggests that both of the Ca^{2+}-binding sites in EF^L are high affinity sites.

3.5. Sequence alignment

We next carried out sequence alignment to assess the experimental results. Both of EF^T and EF^L belong to the canonical EF-hand motif [12]. The canonical EF-hand motif has six calcium ligation residues, which have a spacing in the amino acid sequence of 1, 3, 5, 7, 9 and 12 (Fig. 4). Asp is preferred for the positions 1, 3 and 5, whereas Glu is highly conserved for the position 12. Generally, Ca^{2+} ions prefer the carboxyl group for chelating. The residues of the position 12 of all the EF-hands in EF^T and EF^L are Glu, which is consistent with the ITC results that suggest that all those EF-hands are capable of binding Ca^{2+}. Conservation of the positions 1, 3 and 5 is lower. The positions 3 and 5 of the 1st EF-hand of EF^T have Asn instead of Asp, so the low affinity site of EF^T may be the 1st EF-hand motif of EF^T.

4. Discussion

In cells, the concentration of calcium ion is strictly regulated by calcium pumps and channels in plasma membranes. In the resting state of cells, the intracellular concentration of Ca^{2+} ($[Ca^{2+}]_i$) is kept at 10^{-8}–10^{-7} M, whereas it is increased up to the order of 10^{-6} M in the activated state [21,22]. In the present report, we demonstrated that both EF^T and EF^L change the conformation depending on Ca^{2+} concentration. The NMR and gel filtration analyses demonstrated the higher order structural change of EF^T as well as that of EF^L, although the structural change of EF^T was less extensive than that of EF^L, as shown by the CD measurements.

The results from the fluorescence and ITC analyses together suggest that the structural change of EF^L is quite sensitive to the increase of Ca^{2+} concentration because EF^L has the two equivalently high affinity sites, which together trigger the conformational change of the EF-hands in EF^L. In contrast, the structural change of

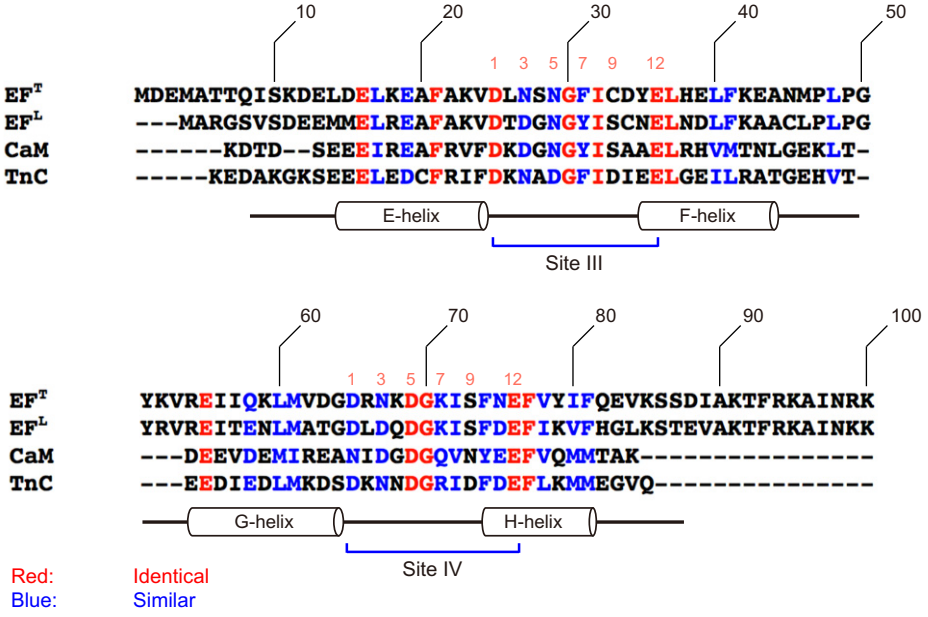

Fig. 4. Sequence alignment of the EF-hand motif from various proteins. The amino acid sequences listed are from T-plastin (EF^T), L-plastin (EF^L) and the C-terminal domains of human calmodulin (CaM) and of turkey skeletal muscle troponin C (TnC). Red and blue characters indicate identical and similar residues among the four sequences, respectively. Numerals at the top (10–100) are the residue numbers of T-plastin. The position numbers (1–12) are those of the Ca^{2+}-chelating residues in the Ca^{2+}-binding loops. The secondary structure representations and nomenclatures below the sequences indicate those of CaM and TnC. The C-terminal domains of CaM and TnC contain E–H helices and Ca^{2+}-binding loops called Sites III and IV [29,30].

EF^T is more modest because one of the Ca^{2+}-binding sites responds modestly to the increase of Ca^{2+} concentration. The sequence alignment shows that the conservation of the acidic residues in the 1st EF-hand of EF^T is lower than the other EF-hands in EF^T and EF^L. These findings suggest that the detailed mechanism by which EF^T changes the structure depending on the Ca^{2+} concentration is different from that by which EF^L does so.

The actin-bundling activity of full length L-plastin is negatively regulated by the elevation of $[Ca^{2+}]_i$ up to approximately 10^{-6} M [16]. Thus, our results using EF^L were consistent with the studies using full length L-plastin. In contrast, full length T-plastin is regulated by 10^{-4}–10^{-3} M Ca^{2+} [23,24], although EF^T changed the conformation by 10^{-5} M Ca^{2+} in our results. This suggests that the propagation of the structural change from EF^T to ABDs of T-plastin is less efficient than that from EF^L to ABDs of L-plastin. $[Ca^{2+}]_i$ is normally elevated up to the order of 10^{-6} M in activated cells, including leukocytes [21,22]. So, L-plastin is capable of changing the structure by typical Ca^{2+} spikes. EF^T is, however, incapable of changing the conformation at typical $[Ca^{2+}]_i$ in activated cells. This is consistent with the observation that T-plastin was insensitive to the Ca^{2+} concentration up to 2.2 μM [25]. One possible *in vivo* condition in which full-length T-plastin would be regulated by calcium is when a cell is disrupted, because the extracellular Ca^{2+} concentration in our body is as high as $\sim 10^{-3}$ M. These evidences together suggest that L-plastin is routinely regulated by $[Ca^{2+}]_i$, whereas T-plastin is normally quite static in cells. Indeed, T-plastin is expressed in unmovable and well-arranged cells, such as epithelial cells and cells of solid organs, in which frequent rearrangement of the cytoskeleton is unnecessary [5–8]. L-plastin is expressed in leukocytes whose morphologies change frequently. Thus, the reason why the T- and L-plastin isoforms are expressed in different kinds of cells may be because the calcium sensitivities of EF^T and EF^L are different.

The expression of L-plastin in cancer cells may be related to the acquired capacity of the cells to migrate and invade. The interaction of cancer cells with extracellular matrix components such as laminin is a key event in tumor invasion and metastasis, and the binding of cancer cells to laminin is known to induce Ca^{2+}-mediated signals in cells [26], suggesting that L-plastin in cancer cells plays a critical role in cellular adhesion and invasion, similar to L-plastin in leukocytes. In fact, down-regulation of L-plastin in cancer cells suppresses their invasion and metastasis [27], whereas up-regulation of L-plastin induces invasion [28].

Acknowledgments

This work was supported in part by Grants-in-Aid for Scientific Research from the Ministry of Education, Culture, Sports, Science, and Technology of Japan. We thank Drs. Hideaki Nojiri and Takashi Umeda at The Biotechnology Research Center, The University of Tokyo for their technical support with the ITC measurements.

Appendix A. Supplementary data

Supplementary data associated with this article can be found, in the online version, at http://dx.doi.org/10.1016/j.bbrc.2012.10.126.

References

[1] T.D. Pollard, J.A. Cooper, Actin and actin-binding proteins. A critical evaluation of mechanisms and functions, Annu. Rev. Biochem. 55 (1986) 987–1035.
[2] V. Delanote, J. Vandekerckhove, J. Gettemans, Plastins: versatile modulators of actin organization in (patho)physiological cellular processes, Acta. Pharmacol. Sin. 26 (2005) 769–779.
[3] S.C. Morley, The actin-bundling protein L-plastin: a critical regulator of immune cell function, Int. J. Cell Biol. 2012 (2012) 935173.
[4] H. Shinomiya, H. Hirata, S. Saito, H. Yagisawa, M. Nakano, Identification of the 65-kDa phosphoprotein in murine macrophages as a novel protein: homology with human L-plastin, Biochem. Biophys. Res. Commun. 202 (1994) 1631–1638.
[5] C.S. Lin, T. Park, Z.P. Chen, J. Leavitt, Human plastin genes, comparative gene structure, chromosome location, and differential expression in normal and neoplastic cells, J. Biol. Chem. 268 (1993) 2781–2792.
[6] J. Leavitt, Discovery and characterization of two novel human cancer-related proteins using two-dimensional gel electrophoresis, Electrophoresis 15 (1994) 345–357.
[7] C.S. Lin, R.H. Aebersold, S.B. Kent, M. Varma, J. Leavitt, Molecular cloning and characterization of plastin, a human leukocyte protein expressed in transformed human fibroblasts, Mol. Cell Biol. 8 (1988) 4659–4668.
[8] M.V. de Arruda, S. Watson, C.S. Lin, J. Leavitt, P. Matsudaira, Fimbrin is a homologue of the cytoplasmic phosphoprotein plastin and has domains homologous with calmodulin and actin gelation proteins, J. Cell Biol. 111 (1990) 1069–1079.
[9] H. Shinomiya, A. Hagi, M. Fukuzumi, M. Mizobuchi, H. Hirata, S. Utsumi, Complete primary structure and phosphorylation site of the 65-kDa macrophage protein phosphorylated by stimulation with bacterial lipopolysaccharide, J. Immunol. 154 (1995) 3471–3478.
[10] S. Banuelos, M. Saraste, K. Djinovic Carugo, Structural comparisons of calponin homology domains: implications for actin-binding, Structure 6 (1998) 1419–1431.
[11] N. Volkmann, D. DeRosier, P. Matsudaira, D. Hanein, An atomic model of actin filaments cross-linked by fimbrin and its implications for bundle assembly and function, J. Cell Biol. 153 (2001) 947–956.
[12] J.L. Gifford, M.P. Walsh, H.J. Vogel, Structures and metal-ion-binding properties of the Ca2$^+$-binding helix-loop-helix EF-hand motifs, Biochem. J. 405 (2007) 199–221.
[13] K. Nakano, K. Satoh, A. Morimatsu, M. Ohnuma, I. Mabuchi, Interactions among a fimbrin, a capping protein, and an actin-depolymerizing factor in organization of the fission yeast actin cytoskeleton, Mol. Biol. Cell 12 (2001) 3515–3526.
[14] M.C. Lebart, F. Hubert, C. Boiteau, S. Venteo, C. Roustan, Y. Benyamin, Biochemical characterization of the L-plastin-actin interaction shows a resemblance with that of alpha-actinin and allows a distinction to be made between the two actin-binding domains of the molecule, Biochemistry 43 (2004) 2428–2437.
[15] V.E. Galkin, A. Orlova, O. Cherepanova, M.C. Lebart, E.H. Egelman, High-resolution cryo-EM structure of the F-actin-fimbrin/plastin ABD2 complex, Proc. Natl. Acad. Sci. USA 105 (2008) 1494–1498.
[16] Y. Namba, M. Ito, Y. Zu, K. Shigesada, K. Maruyama, Human T cell L-plastin bundles actin filaments in a calcium-dependent manner, J. Biochem. 112 (1992) 503–507.
[17] C.S. Lin, W. Shen, Z.P. Chen, Y.H. Tu, P. Matsudaira, Identification of I-plastin, a human fimbrin isoform expressed in intestine and kidney, Mol. Cell Biol. 14 (1994) 2457–2467.
[18] M. Tanokura, K. Yamada, Heat capacity and entropy changes of calmodulin induced by calcium binding, J. Biochem. 95 (1984) 643–649.
[19] F. Delaglio, S. Grzesiek, G.W. Vuister, G. Zhu, J. Pfeifer, A. Bax, NMRPipe: a multidimensional spectral processing system based on UNIX pipes, J. Biomol. NMR 6 (1995) 277–293.
[20] Y. Ogawa, Calcium binding to troponin C and troponin: effects of $Mg2^+$, ionic strength and pH, J. Biochem. 97 (1985) 1011–1023.
[21] E. Donnadieu, G. Bismuth, A. Trautmann, Calcium fluxes in T lymphocytes, J. Biol. Chem. 267 (1992) 25864–25872.
[22] J.T. Myers, J.A. Swanson, Calcium spikes in activated macrophages during Fcgamma receptor-mediated phagocytosis, J. Leukocyte Biol. 72 (2002) 677–684.
[23] D. Zhou, M.S. Mooseker, J.E. Galan, An invasion-associated Salmonella protein modulates the actin-bundling activity of plastin, Proc. Natl. Acad. Sci. USA 96 (1999) 10176–10181.
[24] D.R. Kovar, C.J. Staiger, E.A. Weaver, D.W. McCurdy, AtFim1 is an actin filament crosslinking protein from *Arabidopsis thaliana*, Plant J. 24 (2000) 625–636.
[25] A. Giganti, J. Plastino, B. Janji, M. Van Troys, D. Lentz, C. Ampe, C. Sykes, E. Friederich, Actin-filament cross-linking protein T-plastin increases Arp2/3-mediated actin-based movement, J. Cell Sci. 118 (2005) 1255–1265.
[26] V. Givant-Horwitz, B. Davidson, R. Reich, Laminin-induced signaling in tumor cells, Cancer Lett. 223 (2005) 1–10.
[27] J. Zheng, N. Rudra-Ganguly, W.C. Powell, P. Roy-Burman, Suppression of prostate carcinoma cell invasion by expression of antisense L-plastin gene, Am. J. Pathol. 155 (1999) 115–122.
[28] E. Foran, P. McWilliam, D. Kelleher, D.T. Croke, A. Long, The leukocyte protein L-plastin induces proliferation, invasion and loss of E-cadherin expression in colon cancer cells, Int. J. Cancer 118 (2006) 2098–2104.
[29] O. Herzberg, M.N. James, Refined crystal structure of troponin C from turkey skeletal muscle at 2.0 A resolution, J. Mol. Biol. 203 (1988) 761–779.
[30] Y.S. Babu, C.E. Bugg, W.J. Cook, Structure of calmodulin refined at 2.2 A resolution, J. Mol. Biol. 204 (1988) 191–204.